Automated classification and thematic mapping of bacterial mats in the North Sea

ASM Shihavuddin, Nuno Gracias and Rafael Garcia
Computer Vision and Robotics (VICOROB)
University of Girona (UDG)
Email: shihavuddin/ngracias/rafael.garcia@udg.edu

Javier Escartin
Equipe de Gosciences Marines
CNRS, Paris, France
Email: escartin@ipgp.fr

Rolf Birger Pedersen
Centre for Geobiology
University of Bergen
Email: Rolf.Pedersen@geo.uib.no

***Abstract*—With the current availability of high quality optical sensors and the advancements of Autonomous Underwater Vehicles (AUVs), it is becoming increasingly accessible to acquire extremely large sets of benthic habitat images. Manual characterization and classification of such large number of images for relevant geological or benthic features can become very difficult and time consuming. This paper presents a novel method for automated segmentation, classification and thematic mapping of bacterial mat from shell chaff and sand, on mosaics created from an image survey on the North Sea. The proposed method uses completed Gabor filter response, grey level co-occurrence matrix (GLCM) and local binary pattern (CLBP) as feature descriptors. After chi-square and Hellinger kernel mapping of feature vector, Probability Density Weighted Mean Distance (PDWMD) is used for classification. Initial segmentation is done using TurboPixels. Our proposed method achieves the highest overall classification accuracy and have moderate execution times compared with the set of methods that are representative of the state-of-the-art in automated classification of seabed images. Our work illustrates that applying automated classification techniques to mosaic composites produces a rapid (in terms of expert annotation time) technique of characterizing benthic areas that can be used to track changes over time.**

I. Introduction

Digital underwater imagery has become a widespread tool for seafloor studies, owing to the rapid advancement in imaging electronics over the past 15 years, and to the valuable information these data provides. Advancements in the analysis of underwater imagery have not kept pace with the improvements in image acquisition systems. For the vast majority of surveys, a human analyst must still inspect every frame from a dataset of underwater images to extract relevant information. Software packages such as CPCe [1], Geotexture [2] have improved the efficiency of such analysis, but human input and control is still required. An automated process for classifying underwater imagery would facilitate the study of benthic habitat by reducing the analysis bottleneck and allowing researchers to take full advantage of large underwater image datasets.

This work is motivated by two recent cruises in the North Sea. The cruises, integrated in the EU/FP7 ECO2 project, surveyed the area overlying the subsurface CO2 storage site of the Utsira formation around the Sleipner platforms. One of the main goals of these expeditions was to test techniques for high resolution optical imaging to create photo mosaics and map bacterial mats on the seafloor associated with fluid outflow. The cruises used a Hugin AUV equipped with a high-resolution digital still camera. Identification of bacterial mats and their spatial distribution may guide studies to determine if associated fluid outflows linked to CO2 escape, or to natural processes. The goal of this work is to automatically classify such large datasets to find out the approximate location of bacterial mats, and distinguish these structures from other features that may show similarities, such as shell chaff, which is widespread in the area.

A few of the most challenging obstacles to classification accuracy of underwater images include: significant intra-class and inter-site variability in the morphology of seabed organisms [3] or structures of interest, complex spatial borders between classes on the seabed, subjective annotation of training data by different analysts, variation in viewpoints, distances, and image quality, limits to spatial and spectral resolution when trying to classify to a free taxonomic scale, partial occlusion of objects due to the three-dimensional structure of the seabed, gradual changes in structures of the classes, lighting artifacts due to wave focusing [4]–[6], and variable optical properties of the water column.

Efforts to automate classification have been made for well over a decade [7], but no single algorithm is yet widely accepted as robust. Moreover, no previous work has directly addressed automated bacterial mat classification as only manual identification of such structures has been attempted e.g Barreyre et. al. [8]. One of the fundamental references in automated benthic classification using optical imagery is the work by Pican et al. [7], where grey level co-occurrence matrix (GLCM) [9] or Kohonen maps [10] are used for feature extraction. This method presents promising results on images with distinct texture features, but is not robust to variance in scale, rotation, illumination and blurring effects in water. Marcos et al. [11], [12] use a feed-forward back-propagation neural network to classify underwater images. They use local binary patterns (LBP) [13] as texture descriptors and normalized chromaticity coordinates (NCC) or mean hue saturation value (HSV) as color descriptor. The limitation of this method is the use of mean HSV or NCC color features which in many cases are not discriminative enough. LBP [13] is also used to do identification of crown of thorns starfish (COTS) by Clement et al. [14]. This method focuses only on one class, treating the substrate and all other benthic organisms as background class.

The work by Johnson-Roberson et al. [15], [16] employs both acoustic and optical imagery for benthic classification.

978-1-4799-0002-2/13/$31.00 ©2013 IEEE

Acoustic features and visual features are classified separately using a support vector machine (SVM) with assigned weights, which are determined empirically. Gleason et al. [17] use color and texture in a two-step algorithm to classify 3 broad cover types. The main drawback of this system is that it needs a specialized camera capable of acquiring narrow spectral band images. Mehta et al. [18] utilize a support vector classifier having pixels as features to do coral reef texture classification for only two classes. The method fails on more realistic conditions of noisy images and under varying illumination. It is also relevant the work of Pizarro et al. [19], based on the use of 'bag-of-visual-words' [20] features. In [19], an image is represented as a collection of visual words obtained using SIFT descriptors. However as the number of visual words increases, the time and hardware requirement increase linearly. In this method an entire image is classified as one class or another. Therefore within-image heterogeneity cannot be classified or quantified. The work by Marcos et al. [21] uses LBP and NCC histogram as feature descriptors and linear discriminant analysis (LDA) as classifier. The method were only tested on two classes of benthic habitats. Moreover, LDA classifier is not able to perform constantly well for varied types of seabed image datasets [22].

The work of Stokes and Deane [23] uses normalized color space and discrete cosine transforms (DCT) to classify benthic images. The final classification is done using their proposed probability density weighted mean distance (PDWMD) [23] from the tail of the distribution. This method is time efficient with good accuracy but requires accurate color correction, which may be disadvantageous on underwater images without controlled lighting. The work of Padmavathi et al. [24] uses kernel principal component analysis (KPCA) to project SIFT feature vector on more distinguishable domain. However, this method lacks proper comparison with other methods in varied datasets. Beijbom et al. [3] propose a novel framework for benthic classification which consists of feature vector generation using maximum response (MR) filter bank [25] and SVM classifier with radial basis function kernel. In this method, multiple patch sizes were used, providing a significant improvement relative to classification accuracy. However the use of multiple patch sizes can be redundant and time consuming.

Our proposed method is an extension of the work by Shihavuddin et al. [22]. This work achieves the highest overall classification accuracy and moderate execution times when compared with other related methods on standard texture and benthic datasets. The method is successfully applied on a large image mosaic of the Red Sea (created using 283 high-resolution digital still images and rendering at 1 mm per pixel covering an area of 19.2 square meters) for the thematic mapping of the reef benthos. However, no segmentation of the images is done before classification. Initial segmentation of the image can simplify the problem of thematic mapping and increase the accuracy (which is demonstrated in the Results section). In the proposed method, this extension has been added and tested for comparison as described below.

II. Steps of the Proposed Framework

Our proposed method consists of eight steps to perform overall thematic mapping of the underwater mosaic images. The mosaic images are obtained by registering and blending large sets of individual images acquired at close range [26]–[29]. 29 high-resolution digital still images are used to create the mosaic and are rendered at 4.05 mm per pixel covering an area of 232.86 square meters. The steps of the proposed method for thematic mapping are given in Figure 1 and discussed in brief below.

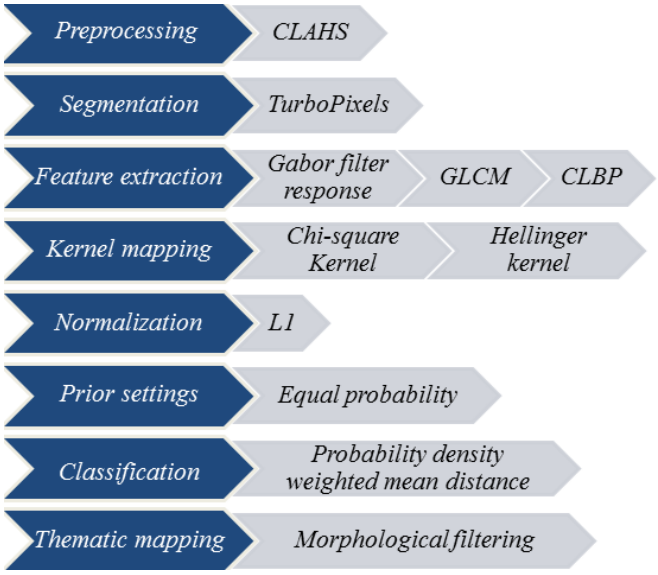

Fig. 1: Steps of the proposed method.

A. Preprocessing

Contrast Limited Adaptive Histogram Specification (CLAHS) [30] is used in the image enhancement step. CLAHS locally enhances the contrast of images by dividing the image into several subregions. This method works very effectively for underwater still images of any size or resolution. For our implementation, we divided the entire image into image patches of size 192 by 192 pixels. Each image patch is then further divided into 4 by 4 subregions and CLAHS is applied on the subregions within each patch.

B. Segmentation

In the proposed method we use a fast superpixels segmentation algorithm called 'TurboPixels' by Levinshtein et al. [31]. Superpixels are dense over-segmentation of an image into lattice-like structure of compact regions that respect local image boundaries. Superpixels reduces image complexity from pixels level to superpixels level through homogeneous pixel grouping while avoiding under-segmentation.

In the TurboPixels method [31], initial seeds are dilated following geometric-flow-based algorithm so as to adapt to local image structure. This method combines a curve evolution model for dilation with a skeletonization process on the background region to prevent the expanding seeds from merging. The algorithm follows the region growing from initial seeds with priorities to maintain uniform size and coverage, connectivity, compactness, smoothness, edge-preserving flow and no overlap of created superpixels. This method performs moderately in terms of compactness, under-segmentation and boundary recall, but it is highly efficient in terms of speed

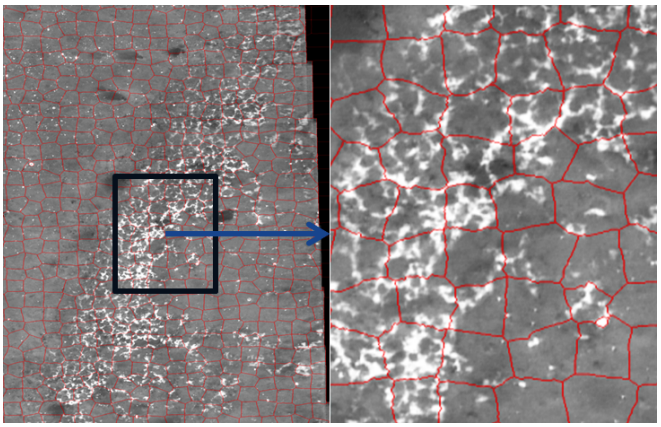

Fig. 2: An example of superpixels segmentation using the TurboPixels method. In the Figure, one pixel covers 16.4025 square millimeters.

(when compared with the other state-of-the-art methods for superpixels segmentation [32]). The number of superpixels can be selected based on the desired amount of over-segmentation of the image. A comparative analysis with varied number of superpixels based on the classification accuracy and time is given in the Results section. Figure 2 shows an example of superpixels segmentation using TurboPixels method on a small part of the mosaic created from the North Sea survey.

C. Feature extraction

The combination of several independent features leads to better image classification results than any single type of feature [33]. In the proposed method we use Gabor filter response [34], grey level co-occurrence matrix (GLCM) [9], [35], [36] and completed local binary pattern (CLBP) [37] as texture feature descriptors. We only used texture features as the raw survey images of North Sea are in grey-scale. In the case of the Gabor filter, by defining 4 sizes and 6 orientations, we obtain 24 images of filter response. Using mean and standard deviation for each of these 24 images, a feature vector of 48 values is created. For GLCM features, we use the 22 features as prescribed in [9], [35], [36]. For CLBP features, we use the rotation invariant format, resulting in a histogram of 108 bins when concatenated for three window sizes of 8, 16, and 24 pixels, respectively.

D. Kernel mapping

Kernel mapping is used to project the feature vectors to linearly separable feature space. We use chi-square and Hellinger kernels in this step as shown in Table I. These two kernel mapping emphasizes low frequent bin counts (containing more discriminative information).

E. Normalization

L1 normalization is applied on the resultant feature vector after kernel mapping to rescale all the features making them comparable.

TABLE I: Chi-square and Hellinger kernel functions. Here h and h' are normalized histograms, where h' is derived from h with first order differentiation. k is the kernel function, γ is the regularization coefficient, i and j corresponds to histogram bin index.

Kernel name	Formulation
Chi-square	$k(h,h^{'}) = \exp\left(-\frac{1}{\gamma}\sum_{j}\frac{\left(h_j - h_j^{'}\right)^2}{h_j + h_j^{'}}\right)$
Hellinger	$k(h,h^{'}) = \sum_i \sqrt{h(i) \times h^{'}(i)}$

F. Prior settings

An estimate of the probability that an image patch will fall into any one of the defined classes can be fused into the classifier. Two choices are possible for estimating this prior probability:

- Class frequency: an existing estimate of the actual class frequency, such as the frequency within the training data,
- Equal probability: by assuming that an image patch has equal probability of falling into any of the defined classes.

In this work, we use equal probability as a prior.

G. Classification

Our algorithm uses probability density weighted mean distance (PDWMD) classifier proposed by Stokes and Deane [23] for classification. Final class labeling of an individual superpixel is done by taking a patch (similar as training patches i.e. 192 by 192 pixels) around the center of the superpixel and classifying that patch. The PDWMD method considers each of the classes in turn and computes Euclidean distances between the sample patch and all training patches for that class (manually created by experts). The mean of the three smallest distances is taken to be the final distance for that class. The final label is determined by choosing the class with the smallest distance.

H. Thematic mapping

The last step of our approach, referred to as thematic mapping, applies the image classification to large area photomosaic of the benthos. This step also includes morphological filter to check for consistency with the neighborhood surrounding each superpixel. Morphological filtering is an effective way of removing misclassifications. The underlying assumption is that each classified superpixel should have at least two superpixels in the 8-neighborhood classified as the same class label. Otherwise, the classified superpixel is re-assigned to the most prominent class label in the 8-neighborhood. A potential drawback of this approach is that the final classification may tend towards dominant, contiguous-cover classes and reduce the representation of classes that are present at small scales (less than superpixel size) and rare (so that they are not contiguous but isolated).

III. Implementation

The proposed method is implemented on the images of the North Sea survey for bacterial mat classification following the flowchart illustrated in 3. This specific North Sea survey image dataset comprises three significant classes: bacterial mat, shell chaff and sand. These classes have been defined beforehand through examination of the imagery from the surveys.

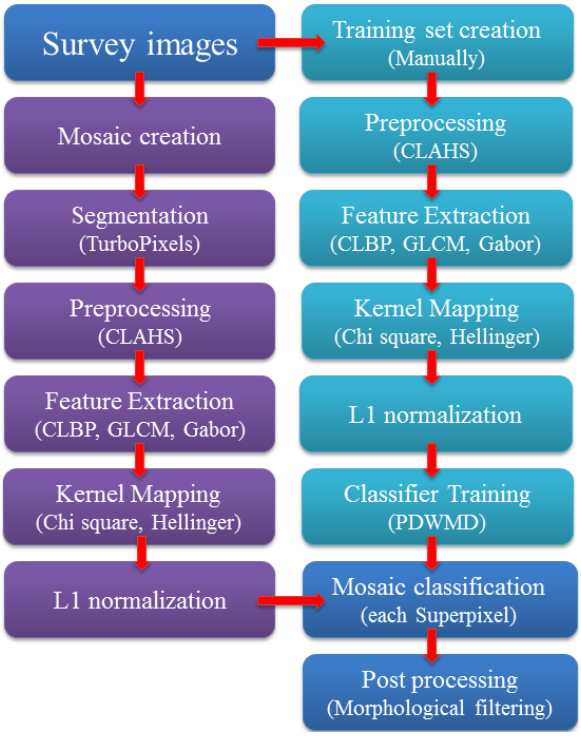

Fig. 3: Flowchart of the implementation of the proposed method.

We use a Hugin dive of the North Sea survey (Dive 10) which comprises almost 37,759 images. Initially the raw survey images are cropped to the size of 1024 by 256 pixels to remove the blurry and noisy portion of the image on the borders. Patches (of 192 by 192 pixels) are extracted from the cropped survey images to be manually annotated by experts creating the training set. Figure 4 shows examples of a single patch from each class. Experts manually classified 24,449 patches (9,625 patches of sand, 14,427 patches of shell chaff and 447 patches of bacterial mat) representing 2.3% of the total number of the image patches of the entire dive 10.

These annotated patches were later preprocessed (CLAHS) and converted into feature vectors as described in the previous section. Thus each image patch is converted into a 178-dimensional feature vector. This feature vector is kernel mapped and normalized as the next step. we use Hellinger kernel and Chi square kernel to emphasis the low frequent bins of CLBP features only. Later we applied L1 normalization on all the features to make them comparable. This way, the image patches are converted into features which represents texture characteristics of the patches. The PDWMD [23] classifier learns class boundaries from this modified feature vector. Equal probability is used as prior for the classifier.

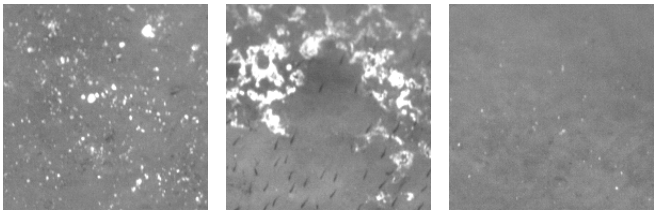

(a) Shell chaff (b) Bacterial mat (c) Sand

Fig. 4: Examples of training patches of each individual class. Each patch is of size 192 by 192 pixels covering an area of 0.6 square meters.

The North Sea mosaic image is obtained by registering and blending individual survey images acquired at close range [26]–[29]. Afterwords, TurboPixels [31] segmentation is applied on the mosaic to simplify it to the superpixels level from the pixels level. Patches around the center of each superpixel are sequentially preprocessed, feature extracted, kernel mapped and normalized (matching the training steps). The earlier trained classifier is used to label each superpixel to the closest class in the training set. On the labeled map, morphological filtering is done to maintain the neighborhood consistency as described in the earlier section.

IV. Results

There is no single method being universally accepted for qualitative assessment of thematic mapping (in some literature referred as spatial simulation model [38], [39]). In general, confusion matrix (referred as error matrix [40] or contingency matrix [39]) contains all the information to calculate quantities for quality assessment. Among these quantities, overall accuracy (OA) [41], kappa (K) [42], average precision (AP), precision-recall (PR) curve and average mutual information (AMI) [43] are being considered in this work. The time required for training and classification is also another important consideration in the presented work.

TABLE II: Comparison of the proposed method with other related state of the art method with respect to overall accuracy (OA), average precision (AP), kappa (K) and time requirement (T).

Method	OA	AP	K	T
Pizarro [19]	73.1%	71.7%	66.3%	9375.6 sec
Beijbom [3]	92.2%	89.5%	84.0%	4892.0 sec
Marcos [11]	87.8%	84.6%	75.4%	**813.1** sec
Stokes [23]	90.1%	89.0.7%	83.5%	1464.6 sec
Proposed method	**99.7%**	**99.6%**	**99.4%**	2611.7 sec

For testing the proposed method and comparing with other related state-of-the-art methods (Pizarro [19], Beijbom [3], Marcos [11] and Stokes & Deane [23]), we use a validation set. The validation set is the exclusive 60% of the training set (randomly selected and not used for training). Table II shows the comparative analysis of these methods based on overall accuracy (OA), average precision (AP), kappa (K) and time requirement (T). The method here achieved much better results than others in terms of accuracy, precision and kappa.

TABLE III: Confusion matrix of our proposed method. The rows show the output class and columns show the ground truth.

	Shell chaff	Bacterial mat	Sand
Shell chaff	**8627 (58.7%)**	0 (0.0%)	11 (0.1%)
Bacterial mat	0 (0.0%)	**265 (1.8%)**	0 (0.0%)
Sand	29 (0.2%)	3 (0.0%)	**5764 (39.2%)**

our method achieved OA of 99.7% where the closest OA is by Beijbom [3] of 92.2%. The time requirement by our method is moderate compared with others. The method by Marcos [11] is the fastest one among related state of the art methods (see Table II).

Figure 5 illustrates the precision recall curves of individual classes using our proposed method on the validation set. In the particular case of bacterial mat class, the average precision was 96.93%, which is less than that of the other two classes. Table III shows the confusion matrix of our proposed method.

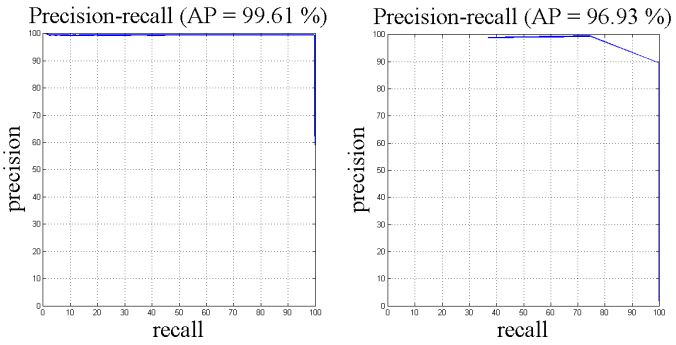

(a) Shell chaff (b) Bacterial mat

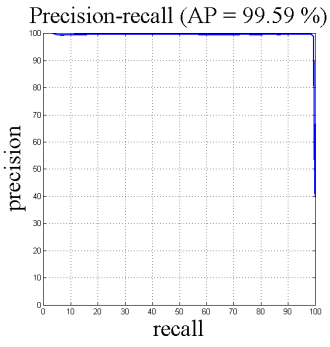

(c) Sand

Fig. 5: Precision recall curves for individual classes using our proposed method on the validation set.

Figure 6 illustrates the classified mapping results of four raw images. In this figure, sand, bacterial mat and shell chaff are labeled in grey, brown and blue, respectively. In this case, only sliding window is being used, without superpixels segmentation.

One important parameter in the segmentation step of our proposed method is the number of superpixels. If the number of super pixels increases, on one hand the resolution of the mapping and the classification accuracy increases. On the other hand, the complexity and the required time increases as well.

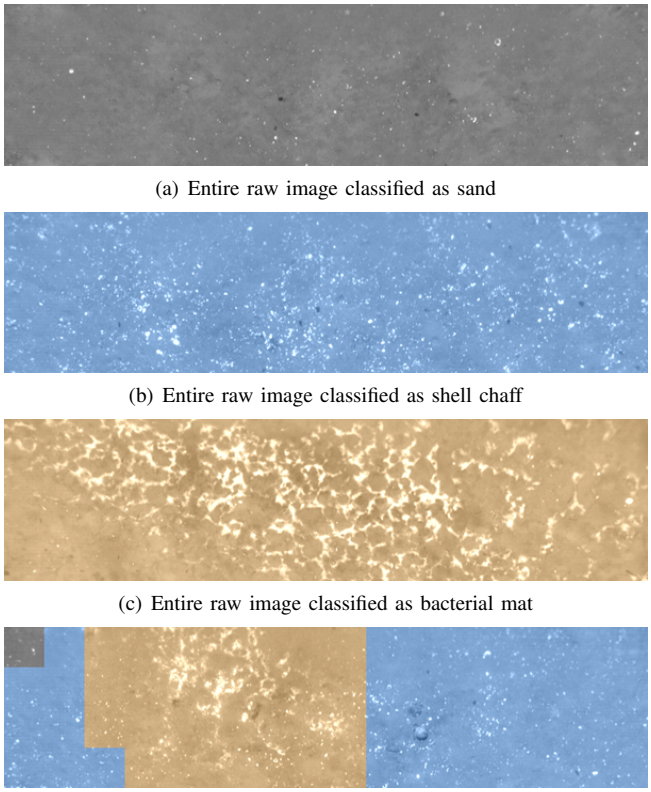

(a) Entire raw image classified as sand

(b) Entire raw image classified as shell chaff

(c) Entire raw image classified as bacterial mat

(d) Raw image classified as mixed of sand, shell chaff and bacterial mat

Fig. 6: Examples of classified raw images dive 10 of North Sea survey images. Each raw image is of size 1024 by 256 pixels at 4.05 mm per pixel.

Experimenting with varied number of superpixels (ranging from 281 to 8,000) created on a mosaic image of size 1,821 by 7,796 pixels, we found that after a certain number of superpixels (approximately 3,000) the classification accuracy is stable but the time required increases linearly with the increase of the number of superpixels (Fig. 7). In our method we used, 2,880 superpixels for the North Sea mosaic image (where the superpixels have approximately the one-ninth of the patch size used for feature detection).

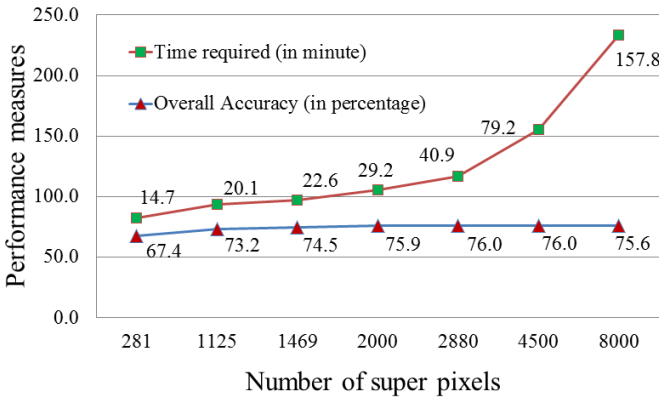

Fig. 7: Effects on varying the number of superpixels.

One of the main contribution of our method is integrating

the superpixels segmentation scheme in the overall thematic mapping framework [22]. We can ascertain that mapping directly on the mosaic image results in better accuracy compared with creating mosaic from classified raw images. This is demonstrated by the experimental results provided in Table IV. In terms of overall accuracy (OA), average precision (AP) and kappa (K), classification performed on mosaic yielded at least 4% more accuracy than that when performed on single images. In terms of average mutual information (AMI), creating the mosaic with classified images increases the performance.

TABLE IV: Comparison based on overall accuracy (OA), average precision (AP), kappa (K) and average mutual information (AMI) between a) Mapping on mosaic images and b) Creating mosaic with classified images.

	Creating mosaic with classified images	**Mapping on mosaic image**
OA	72.3%	**76.0%**
AP	70.8%	**75.1%**
K	59.7%	**63.0%**
AMI	**0.68**	0.61

Figure 8 illustrates the thematic mappings created using both our methods and the ground truth. In this figure, sand, bacterial mat and shell chaff are labeled in grey, brown and blue, respectively, as in prior images. The ground truth is manually created by experts annotating each of the superpixels individually.

The main reasons to apply thematic mapping directly on the mosaic image are:

- The blending of the registered images [26]–[29] partially removes artifacts and noise from the mosaic image.
- Some of the objects are only partially present in the raw images. However in the mosaic they are fully imaged.
- Classifying directly on the mosaic can save a significant amount of resources in terms of time and hardware requirements. In this approach, one object is classified only once ensuring there is no redundancy.
- Better accuracy is achieved when thematic mapping is done directly on the mosaic image.
- Experts get a broader perspective (during annotation) of a patch class on the mosaic facilitating the interpretation and analysis.

V. Conclusion

The importance of this work is emphasized by the fact that autonomous classification will enable characterization of benthic environments across wide areas, using fewer resources in terms of human effort and time and efficiently guiding analysis of large image mosaics. Automatically generated thematic maps of large benthic areas can adapt into a useful tool for experts providing them with valuable information for benthic habitat monitoring, deep water geological exploration, mapping of archaeological sites, supervision of geothermal and volcanic activities, or area monitoring after sudden impacts from natural catastrophes or human impact. This paper contributes to the field by demonstrating the effectiveness of automated classification and thematic mapping with high accuracy for the particular case of bacterial mats in sedimented seafloor, an environment where the numbers of classes are few and each class possesses distinguishable texture features and sufficient training examples. The proposed method is able to classify patches on the mosaic with higher accuracy than other available methods. The framework, experimental results and analysis of this paper constitute an important achievement towards this goal.

VI. Acknowledgments

This work is partially funded by the Spanish MICINN under grant CTM2010-15216 (MuMap), by the EU Project FP7-ICT-2011-288704 (MORPH), and by the FP7-OCEAN.2013.3-265847 (ECO2) and the center for Geobiology of the University of Bergen. ASM Shihavuddin was supported by the MICINN under the FI program. Nuno Gracias was funded by EU Project FP7-INFRASTRUCTURES-2012-312762 (EUROFLEETS2). We would like to thank Oscar Beijbom for making his implementation publicly available on the web and also the authors of Weka, CLBP, Prtools and Vlfeat toolboxes.

References

[1] K. E. Kohler and S. M. Gill, "Coral point count with excel extensions (cpce): A visual basic program for the determination of coral and substrate coverage using random point count methodology," *Computers Geosciences*, vol. 32, no. 9, pp. 1259 – 1269, 2006.

[2] "Geotexture side scan sonar software," *Great Yarmouth, United Kingdom*. [Online]. Available: www.km.kongsberg.com/geoacoustics

[3] O. Beijbom, P. J. Edmunds, D. I. Kline, B. G. Mitchell, and D. Kriegman, "Automated annotation of coral reef survey images," in *IEEE Conference on Computer Vision and Pattern Recognition (CVPR)*, Providence, Rhode Island, 2012.

[4] N. Gracias, S. Negahdaripour, L. Neumann, R. Prados, and R. Garcia, "A motion compensated filtering approach to remove sunlight flicker in shallow water images," in *OCEANS 2008*, Sept. 2008, pp. 1 –7.

[5] Y. Y. Schechner and N. Karpel, "Attenuating natural flicker patterns," in *IEEE / MTS OCEANS Conference*, 2004.

[6] A. S. M. Shihavuddin, N. Gracias, and R. Garcia, "Online sunflicker removal using dynamic texture prediction." in *International Joint Conference on Computer Vision, Imaging and Computer Graphics Theory and Applications (VISAPP)*. SciTePress, 2012, pp. 161–167.

[7] N. Pican, E. Trucco, M. Ross, D. Lane, Y. Petillot, and I. Tena Ruiz, "Texture analysis for seabed classification: co-occurrence matrices vs. self-organizing maps," in *OCEANS '98 Conference Proceedings*, vol. 1, Sep-1 Oct 1998, pp. 424 –428 vol.1.

[8] T. Barreyre, J. Escartn, R. Garcia, M. Cannat, E. Mittelstaedt, and R. Prados, "Structure, temporal evolution, and heat flux estimates from the lucky strike deepsea hydrothermal field derived from seafloor image mosaics," *Geochemistry, Geophysics, Geosystems*, vol. 13, no. 4, 2012.

[9] R. M. Haralick, K. Shanmugam, and I. Dinstein, "Textural features for image classification," *Systems, Man and Cybernetics, IEEE Transactions on*, vol. SMC-3, no. 6, pp. 610 –621, Nov. 1973.

[10] T. Heskes, "Energy functions for self-organizing maps," in *Kohonen Maps*, E. Oja and S. Kaski, Eds. Amsterdam: Elsevier, 1999, pp. 303–315.

[11] M. Marcos, S. Angeli, L. David, E. Peaflor, V. Ticzon, and M. Soriano, "Automated benthic counting of living and non-living components in ngedarrak reef, palau via subsurface underwater video," *Environmental Monitoring and Assessment*, vol. 145, pp. 177–184, 2008.

[12] M. Soriano, S. Marcos, C. Saloma, M. Quibilan, and P. Alino, "Image classification of coral reef components from underwater color video," in *OCEANS, 2001. MTS/IEEE Conference and Exhibition*, vol. 2, 2001, pp. 1008 –1013 vol.2.

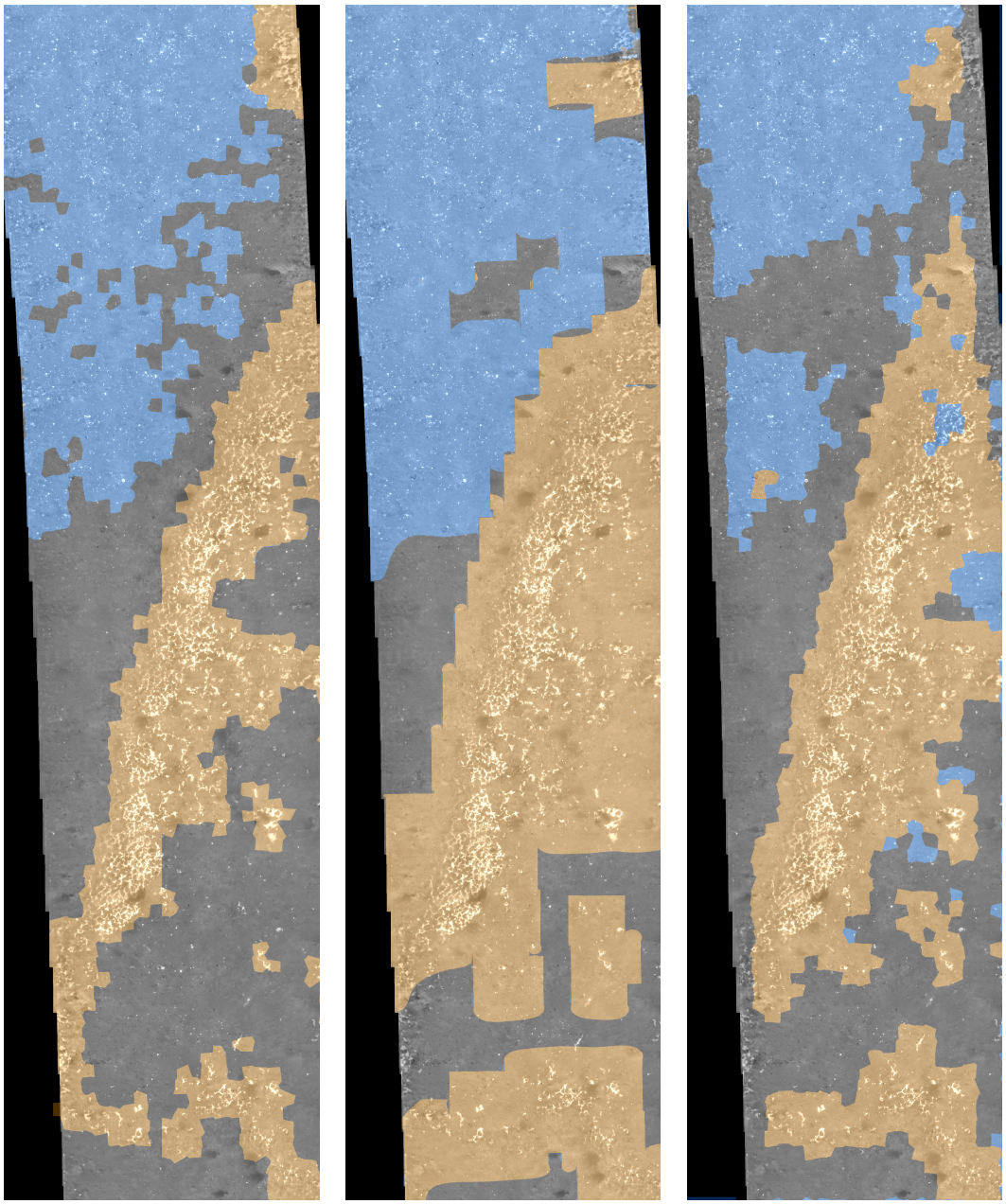

(a) Ground truth

(b) Creating mosaic with classified images

(c) Mapping on the mosaic image

Fig. 8: Thematic mapping results comparison. In the figure sand, bacterial mat and shell chaff are labeled in grey, brown and blue respectively. The mosaic covers an area of 232.86 square meters having width of 7.38 meters and height of 31.5738 meters.

[13] T. Ojala, M. Pietikäinen, and D. Harwood, "A comparative study of texture measures with classification based on featured distributions," *Pattern Recognition*, vol. 29, no. 1, pp. 51–59, Jan. 1996.

[14] R. Clement, M. Dunbabin, and G. Wyeth, "Toward robust image detection of crown-of-thorns starfish for autonomous population monitoring," in *Australasian Conference on Robotics & Automation*, 2005.

[15] M. Johnson-Roberson, S. Kumar, and S. Willams, "Segmentation and classification of coral for oceanographic surveys: A semi-supervised machine learning approach," in *OCEANS 2006 - Asia Pacific*, May 2006.

[16] M. Johnson-Roberson, S. Kumar, O. Pizarro, and S. Willams, "Stereoscopic imaging for coral segmentation and classification," in *OCEANS 2006*, Sept. 2006, pp. 1 –6.

[17] A. Gleason, R. Reid, and K. Voss, "Automated classification of underwater multispectral imagery for coral reef monitoring," in *OCEANS 2007*, 29 2007-Oct. 4 2007, pp. 1 –8.

[18] A. Mehta, E. Ribeiro, J. Gilner, and R. van Woesik, "Coral reef texture classification using support vector machines," in *International Joint Conference on Computer Vision, Imaging and Computer Graphics Theory and Applications (VISAPP), 07*, 2007, pp. 302–310.

[19] O. Pizarro, P. Rigby, M. Johnson-Roberson, S. Williams, and J. Colquhoun, "Towards image-based marine habitat classification," in *OCEANS 2008 Quebec*, Sept. 2008.

[20] T. Serre, L. Wolf, and T. Poggio, "Object recognition with features inspired by visual cortex," in *IEEE Conference on Computer Vision*

and Pattern Recognition (CVPR), vol. 2, June 2005, pp. 994 – 1000 vol. 2.

[21] M. Marcos, M. Soriano, and C. Saloma, "Classification of coral reef images from underwater video using neural networks," *Optics Express*, no. 13, pp. 8766–8771, 2005.

[22] A. Shihavuddin, N. Gracias, R. Garcia, A. C. R. Gleason, and B. Gintert, "Image-based coral reef classification and thematic mapping," *Remote Sensing*, vol. 5, no. 4, pp. 1809–1841, 2013. [Online]. Available: http://www.mdpi.com/2072-4292/5/4/1809

[23] M. D. Stokes and G. B. Deane, "Automated processing of coral reef benthic images," in *Limnol. Oceanogr. Methods*, vol. 7, 2009, pp. 157 –168.

[24] G. Padmavathi, M. Muthukumar, and S. Thakur, "Kernel principal component analysis feature detection and classification for underwater images," in *Image and Signal Processing (CISP), 2010 3rd International Congress on*, vol. 2, Oct. 2010, pp. 983 –988.

[25] M. Varma and A. Zisserman, "A statistical approach to texture classification from single images," *International Journal of Computer Vision*, vol. 62, no. 1-2, pp. 61–81, Apr. 2005.

[26] D. Lirman, N. Gracias, B. Gintert, A. C. R. Gleason, G. Deangelo, M. Gonzalez, E. Martinez, and R. P. Reid, "Damage and recovery assessment of vessel grounding injuries on coral reef habitats using georeferenced landscape video mosaics," *Limnology and Oceanography: Methods*, vol. 8, pp. 88–97, 2010.

[27] J. Escartin, R. Garcia, O. Delaunoy, J. Ferrer, N. Gracias, A. Elibol, X. Cufi, L. Neumann, D. J. Fornari, S. E. Humphris, and J. Renard, "Globally aligned photomosaic of the lucky strike hydrothermal vent field: Release of georeferenced data, mosaic construction, and viewing software," *Geochem. Geophys. Geosyst.*, vol. 9, no. 12, 2008.

[28] D. Lirman, N. Gracias, B. Gintert, A. Gleason, R. Reid, S. Negahdaripour, and P. Kramer, "Development and application of a video-mosaic survey technology to document the status of coral reef communities," *Environmental Monitoring and Assessment*, vol. 125, no. 1-3, pp. 59–73, 2007.

[29] R. Prados, R. Garcia, N. Gracias, J. Escartin, and L. Neumann, "A novel blending technique for underwater gigamosaicing," *Oceanic Engineering, IEEE Journal of*, vol. 37, no. 4, pp. 626–644, 2012.

[30] K. Zuiderveld, "Graphics gems iv," P. S. Heckbert, Ed. San Diego, CA, USA: Academic Press Professional, Inc., 1994, ch. Contrast limited adaptive histogram equalization, pp. 474–485.

[31] A. Levinshtein, A. Stere, K. Kutulakos, D. Fleet, S. Dickinson, and K. Siddiqi, "Turbopixels: Fast superpixels using geometric flows," *Pattern Analysis and Machine Intelligence, IEEE Transactions on*, vol. 31, no. 12, pp. 2290–2297, 2009.

[32] A. Schick, M. Fischer, and R. Stiefelhagen, "Measuring and evaluating the compactness of superpixels," in *Pattern Recognition (ICPR), 2012 21st International Conference on*, 2012, pp. 930–934.

[33] P. Gehler and S. Nowozin, "On feature combination for multiclass object classification," in *2009 IEEE 12th International Conference on Computer Vision (ICCV)*, 29 2009-Oct. 2 2009, pp. 221 –228.

[34] G. Haley and B. Manjunath, "Rotation-invariant texture classification using a complete space-frequency model," *Image Processing, IEEE Transactions on*, vol. 8, no. 2, pp. 255 –269, Feb 1999.

[35] L. Soh and C. Tsatsoulis, "Texture analysis of sar sea ice imagery using gray level co-occurrence matrices," *Geoscience and Remote Sensing, IEEE Transactions on*, vol. 37, no. 2, pp. 780–795, 1999.

[36] D. A. Clausi, "An analysis of co-occurrence texture statistics as a function of grey level quantization," *Canadian Journal of Remote Sensing*, vol. 28, no. 1, pp. 45–62, 2002.

[37] Z. Guo, L. Zhang, and D. Zhang, "A completed modeling of local binary pattern operator for texture classification," *IEEE Transaction on Pattern Analysis and Machine Intelligence*, vol. 19, no. 6, pp. 1657 –1663, June 2010.

[38] G. M. Foody, "Thematic map comparison: Evaluating the statistical significance of differences in classification accuracy," *Photogrammetric engineering and remote sensing*, vol. 70, no. 5, pp. 627–633, 2004.

[39] P. Couto, "Assessing the accuracy of spatial simulation models," *Ecological Modelling*, vol. 167, no. 2, pp. 181 – 198, 2003.

[40] C. Liu, P. Frazier, and L. Kumar, "Comparative assessment of the measures of thematic classification accuracy," *Remote Sensing of Environment*, vol. 107, no. 4, pp. 606 – 616, 2007.

[41] M. Story and R. G. Congalton, "Accuracy assessment - a user's perspective," *Photogrammetric Engineering and Remote Sensing*, vol. 52, no. 3, pp. 397–399, Mar. 1986.

[42] J. Cohen, "A Coefficient of Agreement for Nominal Scales," *Educational and Psychological Measurement*, vol. 20, no. 1, pp. 37–46, Apr. 1960.

[43] J. T. Finn, "Use of the average mutual information index in evaluating classification error and consistency," *International Journal of Geographical Information Systems*, vol. 7, no. 4, pp. 349–366, 1993.